# A new double structure model for expansive clays

Giulia M. Ghiadistri, David M. Potts, Lidija Zdravković & Aikaterini Tsiampousi
*Imperial College London, Civil & Environmental Engineering*

ABSTRACT: The behaviour of compacted bentonite upon hydration is numerically investigated here by simulating a swelling pressure test on a MX-80 bentonite sample. Two constitutive models are employed in the analysis: the "Imperial College Single-Structure Model" (ICSSM) and the "Imperial College Double-Structure Model" (ICDSM), the latter specifically developed for expansive clays. It is shown that the latter exhibits a considerably improved performance as it is able to accurately capture the swelling pressure developed in the material upon wetting. Nevertheless, a limited knowledge of the evolution of the material's fabric, notably at the micro-scale, is an obstacle for deriving with certainty some of the model parameters. This issue is highlighted here by performing analyses of the swelling pressure test with two sets of material characterisations, with model parameters differing in the derivation of the microstructural component. Both analyses show a very good match with the test data, but it is difficult to justify one set of microstructural parameters over the other. The paper emphasises what aspects of experimental research could be helpful in studying the fabric of compacted bentonite upon wetting, and hence improve the calibration procedure of the double-structure model.

## 1 INTRODUCTION

Modelling unsaturated, highly expansive clays is an important and challenging subject of research that entails a vast range of engineering applications, notably an engineered disposal of nuclear waste.

A new constitutive model for expansive clays, called ICDSM, has been developed at Imperial College, which includes a double-porosity structure in its formulation. This new model is used here to study a swelling pressure test on MX-80 bentonite, carried out by Dueck et al. (2011, 2014), which had the purpose of recreating the expansion upon wetting of the material in a controlled laboratory environment. The experiment consists of a constant volume saturation followed by a swelling phase.

The numerical results obtained with the new model are compared with the experimental data, as well as with the results obtained simulating the same test with the ICSSM by Georgiadis et al. (2003, 2005). This model was formulated as an enhancement of the original Barcelona Basic Model (BBM, Alonso et al., 1990), by incorporating a versatile yield surface, a nonlinear increase of apparent cohesion with suction and a nonlinear isotropic compression curve.

While it is reasonable to expect a substantial improvement in the predictions obtained with the double-structure model in comparison to the model by Georgiadis et al. (2003, 2005), some uncertainties regarding the calibration of the model still persist. In particular, the knowledge of the fabric, especially at the micro-scale, is limited due to the lack of experimental evidence and it is foreseeable to further modify the numerical framework once more experimental data becomes available.

## 2 OVERVIEW OF THE NEW MODEL

Two stress variables are used in this framework. One is the equivalent stress, $\sigma = \sigma_{net} + s_{air}$, where $\sigma_{net}$ is net stress, defined as $\sigma_{net} = \sigma_{tot} - p_{atm}$, $\sigma_{tot}$ being total stress and $p_{atm}$ being the atmospheric pressure, which is considered constant; meanwhile, $s_{air}$ is the suction air entry value, which is also assumed to be a constant. The second stress variable is equivalent suction, $s_{eq} = s - s_{air}$, $s$ being the matric suction. The convenience of choosing these stress variables is further discussed in Georgiadis et al., (2003, 2005).

The model takes into account the double-porosity structure, typical of compacted expansive clays, by introducing two interactive scales of structure: the macrostructure and the microstructure. The fabric is

characterised through a model parameter labeled "the void factor", defined as the ratio of microstructural void ratio, $e_m$, over the total void ratio, $e$:

$$VF = \frac{e_m}{e} \tag{1}$$

For the sake of consistency, the following condition must always be satisfied: $e = e_M + e_m$, where $e_M$ is the macrostructural void ratio. Thus, the void factor expresses whether the fabric of the material is predominantly influenced by the microstructure or by the macrostructure.

In accordance with experimental evidence, the microstructure is assumed to be elastic and saturated and its behaviour is purely volumetric. Consequently, the effective stress principle holds and the material behaviour at this level is controlled by the mean microstructural effective stress, defined as:

$$p' = p + s_{eq} \tag{2}$$

where $p$ is the mean equivalent stress. Similar to the assumption in the Barcelona Expansive Model (BExM, Gens & Alonso, 1992; Alonso et al. 1999; Sanchez et al. 2005), the change in microstructural effective stress triggers both reversible and irreversible strains. At microstructural level the elastic strains are quantified as follows:

$$\Delta\varepsilon_m^e = \frac{\Delta p'}{K_m} \tag{3}$$

where the microstructural bulk modulus is defined as:

$$K_m = \frac{1+e_m}{\kappa_m} p' \tag{4}$$

$\kappa_m$ is the elastic compressibility parameter of the microstructure. The material's elastic behaviour upon changes of equivalent stress and/or equivalent suction is defined by contributions from both the macrostructure and the microstructure. The introduced void factor, $VF$, is used here to weigh the contribution of each term, hence obtaining the following total elastic strains due to changes in equivalent suction:

$$\Delta\varepsilon_s^e = \left(\frac{VF}{K_m} + \frac{1-VF}{K_s^M}\right)\cdot \Delta s_{eq} \tag{5}$$

where $K_s^M$ is the macrostructural bulk modulus with respect to changes in equivalent suction and it is defined as follows:

$$K_s^M = \frac{1+e_M}{\kappa_s}(s_{eq} + p_{atm}) \tag{6}$$

$\kappa_s$ being the elastic compressibility of the macrostructure with respect to changes in equivalent suction. Moreover, the global bulk modulus with respect to changes in equivalent stress is:

$$K_{bulk} = \frac{1}{\frac{VF}{K_m} + \frac{1-VF}{K_\sigma^M}} \tag{7}$$

where $K_\sigma^M$ is the macrostructural bulk modulus with respect to changes in equivalent stress, which is defined as:

$$K_\sigma^M = \frac{1+e_M}{\kappa} \mathrm{p} \tag{8}$$

$\kappa$ being the elastic compressibility of the macrostructure with respect to changes in equivalent stress. Finally, Young's modulus is evaluated as:

$$E = 3K_{bulk}(1-2\nu) \tag{9}$$

where $\nu$ is Poisson's ratio. With these components the elastic constitutive matrix can be formed.

Microstructural plastic strains are assumed to be equal to the elastic micro-strains multiplied by a scalar, $f_\beta$, which presents the interaction function:

$$\Delta\varepsilon_\beta^p = f_\beta \Delta\varepsilon_m^e \tag{10}$$

The expression for $f_\beta$ of Sanchez et al. (2005) is adopted, but expanded to allow for the study of boundary value problems:

$$f_\beta = \begin{cases} \begin{cases} c_{c1}+c_{c2}\left(\frac{p_r}{p_0}\right)^{c_{c3}} & if \quad \frac{p_r}{p_0}\geq 0 \\ c_{c1} \quad if \quad \frac{p_r}{p_0}<0 \end{cases} & micro-compression \\ \begin{cases} c_{s1}+c_{s2}\left(1-\frac{p_r}{p_0}\right)^{c_{s3}} & if \quad \frac{p_r}{p_0}\geq 0 \\ c_{s1}+c_{s2} \quad if \quad \frac{p_r}{p_0}<0 \end{cases} & micro-swelling \end{cases} \tag{11}$$

where $c_{c1}$,$c_{c2}$,$c_{c3}$ and $c_{s1}$,$c_{s2}$,$c_{s3}$ are shape coefficients and the ratio $p_r/p_0$ is an expression of the degree of openness of the structure (Gens and Alonso, 1999), as it takes into account the distance of the current stress state from the yield surface. The $p_0$ is the isotropic yield stress and $p_r$ is related to the current stress state.

At every loading step, one of the $f_\beta$ functions from Equation (11) is active, depending on whether the microstructure is swelling or contracting, which is established according to the sign of the microstructural effective stress change. However, this selection is not a simple task because the integration of the constitutive model equations to obtain the change in mean microstructural effective stress, $\Delta p'$, from changes in total strains, $\Delta\varepsilon$, requires prior knowledge of its value (i.e. $\Delta p'$ is an unknown in the iterative solution of governing equations). Consequently, an alternative criterion from that reported in the literature is adopted here, which relies on the to-

tal strain changes when selecting the active interaction function:

1. $\Delta\varepsilon_{vol} \geq 0 \rightarrow$ micro-swelling
2. $\Delta\varepsilon_{vol} < 0 \rightarrow$ micro-compression

where $\Delta\varepsilon_{vol}$ is the change in volumetric total strain. This adjustment in the formulation allows the implementation of the model in a general finite element software, required to solve boundary value problems.

Thus, the model allows the contribution of the microstructure in the irreversible behaviour to be included in a relatively simple conceptual manner. However, this complicates the formulation because the microstructural plastic mechanism cannot be associated with a proper yield surface and, hence, it cannot be defined within the classical plasticity theory. All details on how this issue has been overcome, as well as the model's implementation in a finite element code, are discussed in Ghiadistri et al. (2018).

Irreversible changes due to loading imply the evolution of the material at both scales. The state of the microstructure is monitored by the void factor, *VF*, which, in the model formulation, acts as a hardening parameter. Its evolution law is defined as follows:

$$\Delta \mathrm{VF} = \frac{\Delta e}{e} \frac{\Delta p'}{K_m \Delta \varepsilon_{vol}} \tag{12}$$

On the other hand, the macrostructure, which is governed by the framework described in Georgiadis et al. (2003, 2005), follows the familiar hardening law of the critical state framework:

$$\Delta p_0^* = p_0^* \frac{\nu}{\lambda(0) - \kappa} \Delta \varepsilon_{vol}^p \tag{13}$$

where $p_0^*$ is the equivalent fully saturated yield stress, $\nu$ is the specific volume, $\lambda(0)$ is the fully saturated compressibility coefficient and $\Delta\varepsilon^p_{vol}$ is the change in plastic volumetric strain. The latter is the sum of two contributions, the macrostructural one, indicated with the subscript LC, and the microstructural one, indicated with the subscript $\beta$:

$$\Delta \varepsilon_{vol}{}^p = \Delta \varepsilon_{vol,LC}^p + \Delta \varepsilon_{vol,\beta}^p \tag{14}$$

As a result, the macrostructural hardening law ensures the coupling between the two structures. However, it should be noted that while the micro-scale influences the evolution of the macrostructure, the opposite does not apply.

Finally, the model takes into account that the fabric of the material undergoes permanent changes upon hydration. This means that the double porosity structure disappears upon full saturation and the material assumes a single porosity structure (Seiphoori et al., 2014; Monroy et al., 2010). Such change is irreversible. Consequently, once the suction has reduced below the air-entry value, the void factor is set to zero and the microstructure ceases to exist. This does not cause any discontinuity in the behaviour of the material because the total void ratio does not present any discontinuity.

## 3 EXPERIMENT

The axial swelling test to be simulated comprises the constant volume saturation of a cylindrical sample, 50mm in diameter and 20mm high, followed by free expansion in the axial direction until an axial strain of 25% is reached. The experimental set-up is shown in Figure 1.

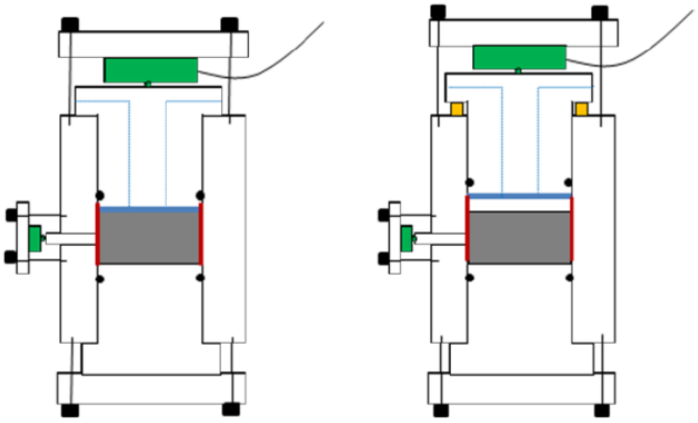

Figure 1. Experimental setup for the axial swelling test (Dueck et al., 2011, 2014).

Throughout the course of the experiment, the sample is confined laterally by means of a steel ring, whereas a piston is placed along its top boundary in order to ensure constant volume conditions before and after the expansion phase. No counteracting shear stresses are present on the lateral boundary as the friction is minimised by use of a lubricant. The wetting boundary coincides with the top of the specimen. Two load cells are placed in the vertical and radial direction, allowing total stresses to be monitored during the entire duration of the tests. In particular, radial pistons are placed in holes through the steel ring for the measurement of radial forces (Dueck et al., 2011, 2014).

The experiment can be divided into the following stages: 1) wetting at constant volume until saturation; 2) piston is moved 5 mm upwards, with no water inflow or outflow allowed. The contact between piston and sample is lost at this stage; 3) bentonite swells and fills the space left by the piston, while allowing inflow or outflow of water; 4) once the sample-piston contact has been re-established, and thus the volume of the sample is again constant, the swelling pressure can be measured again.

## 4 NUMERICAL SIMULATION

### 4.1 *Analysis, material and initial conditions*

The simulation of this experiment is performed with a finite element code ICFEP (Potts & Zdravkovic, 1999), the bespoke computational platform of the Geotechnics research group at Imperial College in which the model is implemented.

The analysis of this experiment requires hydro-mechanically coupled formulation. It is carried out using a finite element mesh consisting of 9 (3x3) quadrilateral, 8-noded finite elements. Due to the geometric and loading symmetry of the experiment, the analysis is performed as axi-symmetric. Additional analyses with finer meshes showed no mesh-dependency of the numerical predictions. The width of the mesh is 25mm and the height 20mm.

The calibration of the double structure model for MX-80 bentonite yields the parameters reported in Table 1; whereas the initial conditions of the specimen are listed in Table 2.

Table 1. Model calibration for MX-80 bentonite.

| Parameters | |
|---|---|
| $\alpha_f = \alpha_g$, 1st shape parameter YS and PP | 0.4 |
| $\mu_f = \mu_g$, 2nd shape parameter YS and PP | 0.9 |
| $M$, stress ratio at critical state | 0.5 |
| $p_c$, Characteristic pressure (kPa) | 1000 |
| $\lambda(0)$, Fully saturated compressibility coefficient | 0.25 |
| $\kappa$, elastic compressibility coefficient, Macro | 0.08 |
| $r$, maximum soil stiffness parameter | 0.61 |
| $\beta$, soil stiffness increase parameter (1/kPa) | 0.00007 |
| $\kappa_s$, elastic compressibility coefficient w.r.t. suction, Macro (kPa) | 0.06 |
| $\nu$, Poisson's ratio | 0.4 |
| $s_0$, yield value of suction (MPa) | 1000 |
| $\kappa_m$, elastic compressibility coefficient, micro (kPa) | 0.18 |
| $c_{s1}$, $c_{s2}$, $c_{s3}$, swelling interaction function coefficients | -0.1,1.1,2 |
| $c_{c1}$, $c_{c2}$, $c_{c3}$, contraction interaction function coefficients | -0.1,1.1,2 |
| $s_{air}$, air-entry value of suction for wetting and drying paths (kPa) | 1000 |

Table 2. Initial conditions.

| Values | |
|---|---|
| Compaction pressure (MPa) | 35 |
| Water content (%) | 12 |
| Void ratio | 0.68 |
| Void factor | 0.4 |
| Dry density (kg/m3) | 1655 |
| Axial stress (MPa) | 0.6 |
| Radial stress (MPa) | 0.3 |

### 4.2 *Boundary conditions*

The boundary conditions applied in the analysis are the following: *phase 1*, horizontal displacements are set to zero along the vertical boundaries of the mesh, while vertical displacements are set to zero at the horizontal boundaries, thus creating a constant-volume conditions. A gradual (reducing) change in suction is imposed on the top boundary until the equivalent suction reaches zero throughout the whole sample in a given time; there is no flow of water across the remaining sample boundaries in all phases of the experiment; *phase 2*, horizontal displacements are set to zero on the vertical boundaries and vertical displacements are set to zero on the bottom boundary. There is now no flow of water across the top boundary of the mesh, as the simulated sample is not in contact with water at this stage. The top boundary is allowed to swell freely, with the vertical reactions at nodes on this boundary, created from the restriction of movements in *phase 1*, gradually reduced to zero; in *phase 3*, a change in suction is further imposed at the top boundary, while horizontal displacements remain set to zero on the vertical boundaries and vertical displacements remain set to zero on the bottom boundary. These boundary conditions apply until the desired heave of the top boundary has been reached; *phase 4*, same boundary conditions as phase 1.

## 5 RESULTS AND DISCUSSION

In Figures 2 and 3 the evolution of the total axial stress and the total radial stress in time is shown, as predicted from the analyses employing the above presented ICDSM and the ICSSM.

The match between experimental data and numerical solution is very good in the case of the expansive model, which predicts a considerably higher axial and radial total stress than the single structure model. Comparing the magnitudes of the stress predicted by the models, it can be argued that the microstructure is responsible for a considerable amount of the swelling. It can also be noticed that, according to the laboratory data, the radial stress reached upon full saturation (10MPa) is slightly higher than the axial stress (8MPa), whereas both models predict an isotropic behaviour. This could suggest that the material presents some anisotropy in its mechanical response, maybe caused by the one-dimensional compaction process that the specimen has undergone before testing. An extensive experimental study would be required to characterise the potential anisotropy of compacted bentonite, based on which it would be possible to adjust the numerical model accordingly.

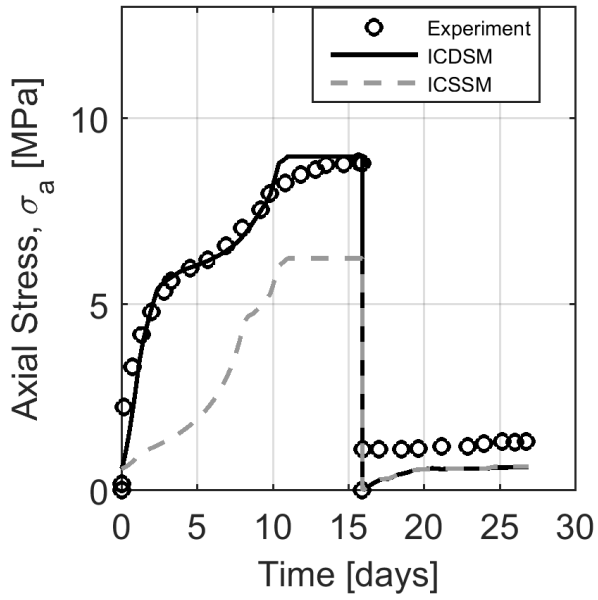


Figure 2. Axial swelling pressure evolution in time from experimental data and numerical predictions. Due to the lack of experimental data, phase 3 is not represented in this figure.

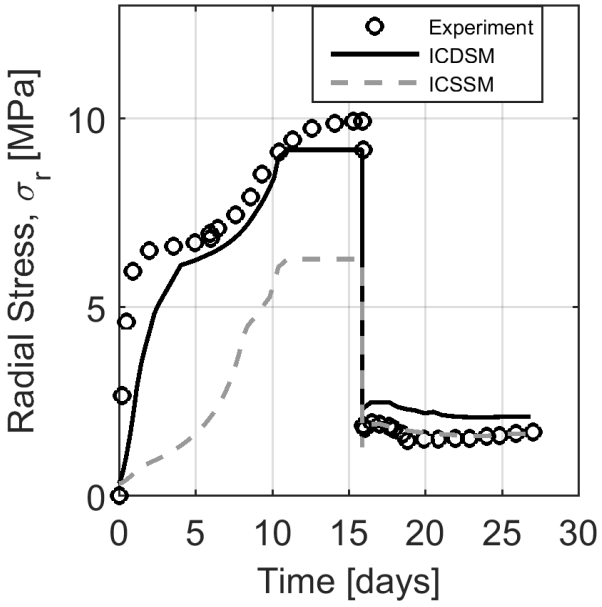


Figure 3. Radial stress evolution in time from experimental data and numerical predictions.

The results of the numerical analysis using the new double-structure model are very encouraging. However, there is a degree of uncertainty regarding the model calibration in relation to the microstructural parameters $f_\beta$ and $\kappa_m$, as they have not been derived from any experimental evidence. At present, such evidence is lacking from laboratory tests. The interaction functions have been shaped on the basis of qualitative considerations, while the microstructural compressibility has been assumed to have a value that is comparable to those typical of elastic compressibility parameters. On the other hand, the other microstructural parameter, the void factor, can, in principle, be quantitatively correlated to results from Mercury Intrusion Porosimetry (MIP) investigations. However, this needs further research to quantify the evolution of microstructural change from the as-compacted double-porosity to the fully saturated single porosity structure.

An example of the likely consequences resulting from the uncertainties in the calibration of the model's microstructure is shown in Figure 4. The figure shows the same measured axial swelling pressure as in Figure 2, and two numerical predictions of this pressure. The prediction "Cal#1" is the same as shown in Figure 2, obtained by employing model parameters in Table 1. The second prediction "Cal#2" is obtained by redistributing the compressibility of the material between the two levels of structure and modifying the interaction functions. The microstructural parameters are changed to $\kappa_m=0.1$ and $c_{c3}=c_{s3}=5.0$, meanwhile the macrostructural compressibility parameter with respect to suction is set to $\kappa_s=0.091$, which is still a realistic value for bentonite. Both predictions show an excellent agreement with the test data. This represents an unusual outcome as the material should be unequivocally characterised. At present there is no sufficient experimental evidence to choose one calibration over the other.

Consequently, as the effectiveness of the new model has been demonstrated, further effort is needed in elaborating a satisfactory calibration process for all of its parameters. It is evident that this requires further experimental investigation of the microstructure of compacted expansive clays. Further experimental information could also lead to reformulating certain aspects of the framework in order to assign a more precise physical meaning to the relevant parameters.

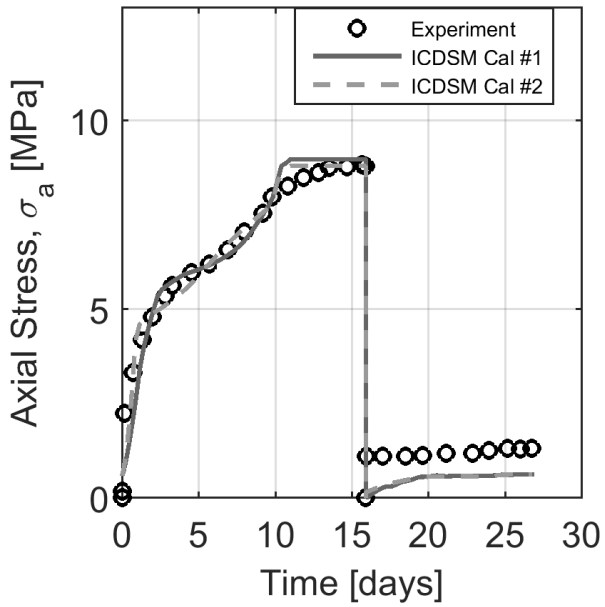


Figure 4. Two alternative calibrations for MX-80 bentonite give equally satisfying results.

## 6 CONCLUSIONS

A new double structure constitutive model for expansive clays is introduced and used to reproduce a swelling test on a compacted sample of MX-80 bentonite. The simulation shows very good results, as the ICDSM clearly improves the model performance compared to that of the ICSSM. The simulations emphasise the relevance and the role of the microstructure in the swelling of highly expansive clays. Nevertheless, some uncertainties about the calibration of the model, mostly due to the lack of experimental evidence regarding the microstructure, still remain and require further testing of this material, with a particular focus on quantifying the evolution of the microstructure in the hydration process.

## 7 ACKNOWLEDGEMENTS

The work presented in this paper is funded by AMEC Foster Wheeler, UK and Radioactive Waste Management Ltd., UK.

## 8 REFERENCES

Alonso, E., Gens, A. & Josa, A. 1990. A constitutive model for partially saturated soils. *Géotechnique* 40(3): 405-430.

Alonso, E., Vaunat, J. & Gens, A. 1999. Modelling the mechanical behaviour of expansive clays. *Engineering Geology* 54(1-2): 173-183.

Dueck, A., Goudarzi, R. & Börgesson, L. 2011. Buffer homogenisation, status report. *SKB Technical Report* TR-12-02.

Dueck, A., Goudarzi, R. & Börgesson, L. 2014. Buffer homogenisation, status report 2. *SKB Technical Report* TR-14-25.

Gens, A. & Alonso, E. 1992. A framework for the behaviour of unsaturated expansive clays. *Canadian Geotechnical Journal* 29(6): 1013-1032.

Georgiadis, K., Potts, D.M. & Zdravković, L. 2003. The influence of partial soil saturation on pile behaviour. *Géotechnique* 53(1): 11-25.

Georgiadis, K., Potts, D.M. & Zdravković, L. 2005. Three-dimensional constitutive model for partially and fully saturated soils. *Int J Geomech* 5(3): 244-255.

Ghiadistri, G.M., Zdravković, L., Potts, D.M. & Tsiampousi, K. 2018. A double structure framework for unsaturated expansive clays. In preparation.

Monroy, R., Zdravković, L., & Ridley, A. 2010. Evolution of microstructure in compacted London Clay during wetting and loading. *Géotechnique* 60(2): 105-119.

Potts D.M. & Zdravkovic L. 1999. *Finite element analysis in geotechnical engineering: theory*. Thomas Telford, London.

Sanchez, M., Gens, A., do Nascimento Guimaraes, L. & Olivella, S. 2005. A double structure generalized plasticity model for expansive materials. *Int. J. Numer. Anal. Meth. Geomech* 29: 751-787.

Seiphoori, A., Ferrari, A. & Laloui, L. 2014. Water retention behaviour and microstructural evolution of MX-80 bentonite during wetting and drying cycles. *Géotechnique* 64(9): 721-734.